MODULATING THE PSEUDOELASTIC RESPONSE OF NITI USING ION IMPLANTATION

Ni-ion irradiated NiTi observed to be nearly 50% harder, retains 85% recoverable deformation, has reduced hysteresis

Alejandro Hinojos[1], Daniel Hong[1], Longsheng Feng[1], Chao Yang[2], Janelle P. Wharry[2], X Gao[1], Khalid Hattar[3], Nan Li[4], Jeremy E. Schaffer[5], Yunzhi Wang[1], Michael J. Mills[1], Peter M. Anderson[1]

[1] Dept. of Materials Science and Engineering, The Ohio State University, Columbus, OH, 43210, USA
[2] School of Materials Engineering, Purdue University, West Lafayette 47906, IN, USA
[3] Center for Integrated Nanotechnologies, Sandia National Laboratories, Albuquerque, NM, 87185, USA
[4] Center for Integrated Nanotechnologies, MPA Div., Los Alamos National Laboratory, Los Alamos, NM 87545 USA
[5] Fort Wayne Metals Research Products, LLC, Fort Wayne, IN, USA 46809

A. Intro

This work explores whether ion beam modification can be used to modulate the austenite to martensite phase transformation in NiTi, thereby achieving novel or localized transformation properties in near-surface regions. This could provide alternatives to laser shot peening or other surface treatment methods and possibly expand applications in biomedical, aerospace, and other fields [1]–[5]. Irradiation induces defects and internal stress that can serve as nucleation and/or pinning sites for the phase transformation. Thus, it can augment more conventional approaches, including alloying [6]–[11], severe mechanical work [12]–[14], grain size reduction [15], and precipitation of coherent precipitates [15], [16]. A range of outcomes is possible in principle, including a shift of the critical stress or temperature for onset of the transformation, linearization, reduction of hysteresis, stabilization, and extent of transformation strain.

Because prior studies show irradiation amorphization of NiTi-based intermetallics [17]–[24], this work employs lower doses of irradiation (< 0.1 DPA, displacements per atom) to retain a large volume fraction of ordered phase, and then uses nanoindentation and structural analysis to probe sub-micron and nano-scale features that are not accessible with conventional or micron-scale pillar testing [25]–[29]. Nanoindentation has the capacity to clearly identify the austenite-martensite phase transformation [30] as well as tension-compression asymmetry and anisotropy [31]–[33].

B. Approach

A combined experimental-computational approach was used to study the hypothesis that irradiation defects can modulate the phase transformation. First, cross sectioned samples of drawn Ti-$Ni_{50.5\%at}$ 3.2 mm diameter wire (Ft. Wayne Metals) with a <111> axial texture were metallographically prepared and irradiated into the top axial surface with 30 MeV Ni^{6+} ions to achieve a fluence of 5 x 10^{13} cm^{-2} using the Tandem Accelerator Facility at the Center for Integrated Nanotechnology at Sandia National Labs [34]. SRIM software [35] was used to specify this fluence to achieve < 0.1 DPA (Displacement per Atom), the critical threshold for amorphization [19].

Next, Berkovich indentation to 250 nm depth on polished side facets was performed with a Hysitron TI950 TriboIndenter at the Center for Integrated Nanotechnologies at Los Alamos National Laboratory [36], to sample submicron volumes $V_{ind} \approx 0.125\ \mu m^3$ at positions z = 0 to 8 µm below the implanted surface. For reference, ~70 indents in unirradiated drawn Ti-$Ni_{50.5\%at}$ wire were performed perpendicular to the <111>

axial texture. Both scanning electron microscopy (SEM) and transmission electron microscopy (TEM) were used for structural characterization. Two simulation methods were used to explore the influence of possible irradiation defects on the martensitic phase transformation. At the submicron scale, phase field (PF) modeling following Zhu et al. [36] and at the atomistic scale molecular dynamics (MD) simulations were used to study stress-induced transformation in 170 nm and 21 nm cubes, respectively, with and without irradiation type defects. The PF simulations applied a compressive stress of 700 MPa along the <100> B2 direction and solved the time-dependent Ginzburg-Landau equation [37] on a 128×128×128 grid. The MD simulations applied a tensile strain of 0.1 at a rate of 0.001 ps^{-1} and used LAMMPS [38] and Ko and coworkers' [39] Modified Embedded Atom Method (MEAM) potential, which accurately captures the B2-B19' transformation, and OVITO [40] for phase identification and common neighbor analysis.

C. Results

The indentation results (Figure 1) show that at z ≈ 3.6 µm below the implantation surface, the irradiated material exhibits an indentation load P_{250nm} = 8.5 mN, ~46% larger than for unirradiated material, yet the recoverable displacement δ_{rec} upon unloading is comparable to unirradiated material. The cycle 2 indentation curves - where the material is reindented at the same site - show that the irradiated material has smaller hysteresis and is more stable, with negligible plasticity, compared to the unirradiated material. Simulated unloading curves for an elastic-plastic material with an elastic modulus of austenite (90 GPa) [41] and a plastic flow strength that is adjusted to match the cycle 1 loading response are computed using a finite element model. The difference, δ_{recPT}, between the simulated and experimental curves denotes the recoverable displacement attributable to the phase transformation. The irradiated material has ≈ 85% of the recoverable displacement of unirradiated material.

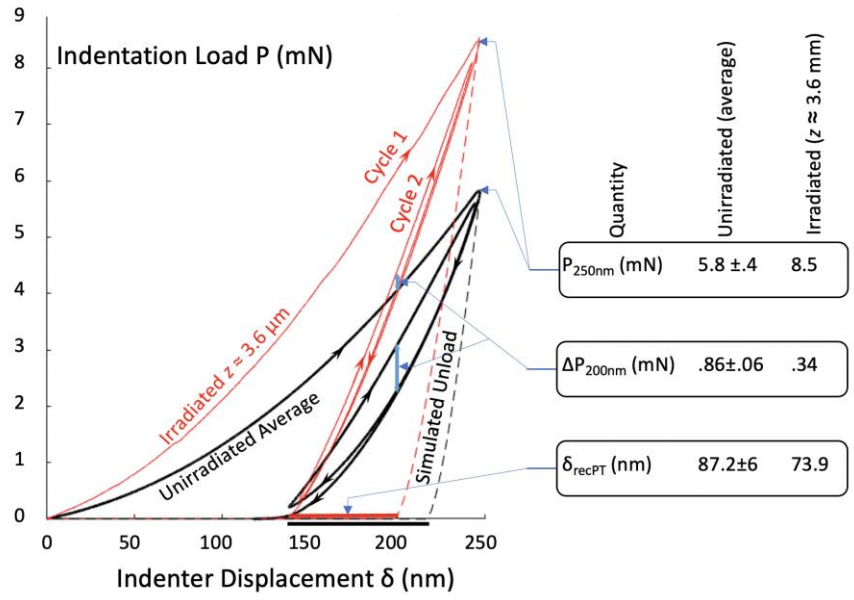

Fig. 1 − Nanoindentation response in unirradiated (averaged over ~70 indentations) and irradiated (single indent location at z ≈ 3.6 µm below the implanted surface) drawn Ti-Ni50.5at% wire.

The SEM electron backscatter diffraction (EBSD) inverse pole figure (IPF) map (Figure 2a) reveals equiaxed grains and a dark band at ~3 µm below the implantation surface, as well as indentation sites in the vicinity of the band. The inability to properly index the band and indentation sites signify damage that could be caused by amorphous regions and other defects cited in prior work. The regions outside the band are still

indexed as crystalline B2 phase but are likely to contain some amorphous damage. Additional evidence from enhanced contrast in backscattered electron (BSE) [42] imaging (not shown) supports the presence of a damage distribution consistent with implantation in other alloys [43]–[45]. The TEM bright field image (Figure 2b) shows a cross-section near one of the indents. The faint traces of defects immediately beneath the indent are likely dislocations generated by indentation. The diffraction pattern inset of the $[111]_{B2}$ reveals azimuthal elongation of the $<110>_{B2}$ spots showing signs of crystal rotation [22] from plasticity or retained internal stresses [46]. Characterization using scanning TEM (S/TEM) bright field imaging (not shown) suggests that pre-existing defects near the damage band can be destroyed, setting the stage for investigation of dislocations in amorphous regions and whether amorphization in the B2 phase is continuous [19], [22].

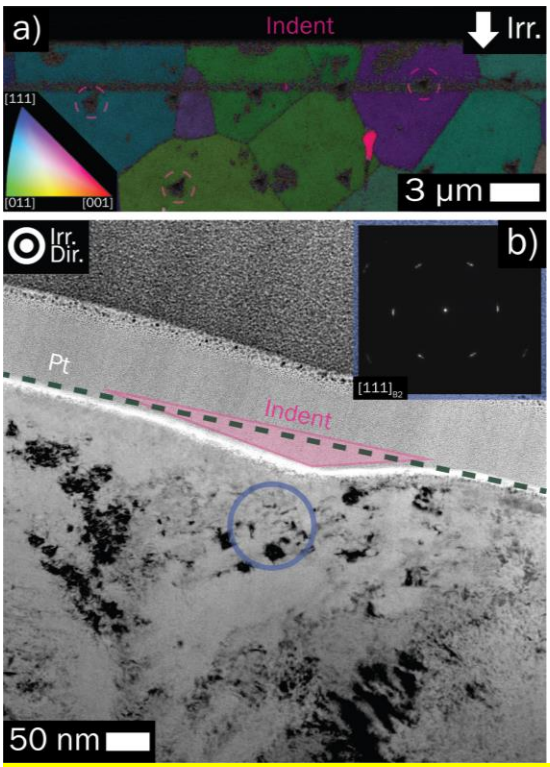

Fig. 2 – (a) EBSD IPF map normal to wire axis; (b) TEM bright field image, cross section of an indent located above the damage band in (a).

The phase field simulations (Figure 3a-e) predict that a B2+amorphous composite with a morphology approximated by S/TEM observations (white = amorphous, black = B2) does not transform to martensite (variants v1-v4 as indicated by colors) as readily as the B2-only case (Figure 3f-j). The B2 phase in the composite is interconnected but the channels cannot be filled fully by self-accommodating martensitic variants. The stark contrast between Figures 3e, j clearly indicate that the autocatalysis of the martensitic transformation has been suppressed by the elastic but non-transforming amorphous phase. This is consistent with the significantly larger nanoindentation load for irradiated NiTi (Figure 1).

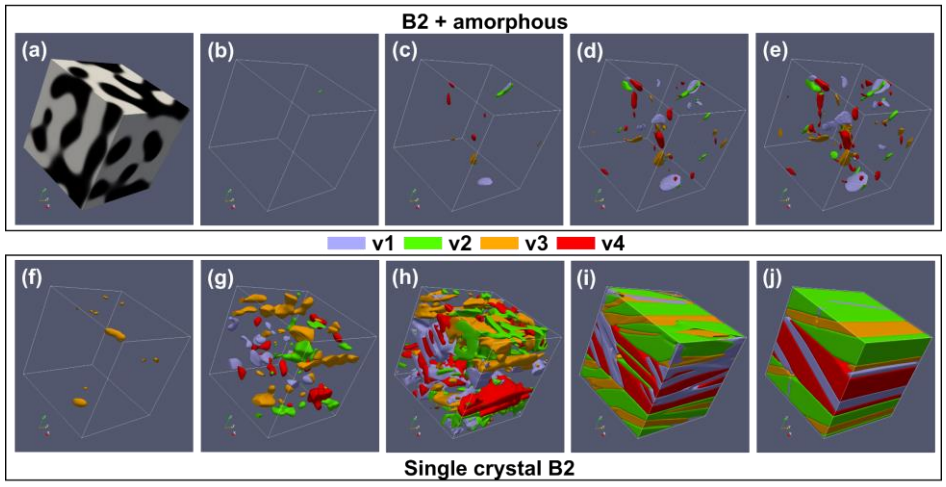

Fig. 3 – Phase field simulations of the B2-B19' transformation in (a-e) a B2(black)+amorphous(white) composite and (f-j) a single B2 crystal without an amorphous structure. The four martensite variants v1, v2, v3 and v4 (see color key) can form self-accommodating herringbone microstructures.

The MD simulations (Figure 4) predict that point defects and defect clusters also hinder the B2-B19' martensitic phase transformation. At a total strain of 0.08 (loading), the pristine B2 structure (Figure

4a) forms an internally-twinned B19′ martensite structure while the simulations with interstitials (Figure 4b) and vacancies (Figure 4c) form the twinned B19′ structure with fewer B19′ transformed lattice sites. The vacancy cluster case (Figure 4d) shows even greater defect-mediated suppression of the transformation and at greater strain (Figure 4e), the vacancy clusters appear to constrain the growth of B19′ martensite (compare insets, Figures 4d, e). The MD results, like the PF counterparts, are consistent with the larger indentation load required for irradiated NiTi. The detailed defect structures are ultimately determined by a balance of free energy, which drives the maintenance of short-range order, and irradiation-induced ballistic disordering of lattice atoms [47].

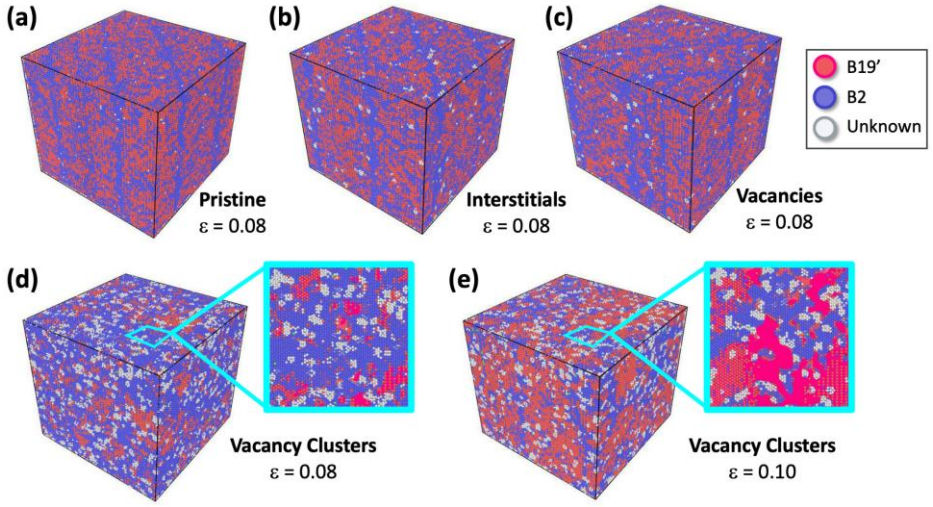

Fig. 4 – Molecular dynamic simulations of the B2-B19′ transformation in equiatomic NiTi for (a) pristine (b) interstitials (10^{-4} at%), (c) vacancies (10^{-4} at%), and (d) vacancy clusters (10^{-3} at%) at 0.08 strain and (e) vacancy clusters (10^{-3} at%) at 0.1 strain. See key for color of lattice sites.

D. Conclusions

Ni ion beam modification of Ti-$Ni_{50.5\%at}$ wire at <0.1 DPA is shown to increase the indentation load in implanted regions by as much as ~50%, yet retain ~85% of recoverable displacement while achieving ~60% reduction in hysteresis, greater stability, and more linear behavior. Electron microscopy reveals inhomogeneously distributed damage consisting of a mixture of amorphous and crystalline B2 phases in the implanted region. The increased hardness is supported by phase field and molecular dynamics simulations that predict defects at multiple scales to require increased load to achieve the B2-B19′ martensitic transformation. The results suggest the potential for Ni ion beam modification to achieve functional surface modification of NiTi.

E. Acknowledgements

Work was supported by the U.S. Department of Energy (DOE), Office of Science, Basic Energy Sciences (BES), at The Ohio State University (OSU) under award #DE-SC0001258 (indentation analysis, characterization, and phase field simulations) and at Purdue University under award #DE-SC0020150 (molecular dynamics simulations). Material–Fort Wayne Metals (Fort Wayne, IN); Irradiation and nanoindentation experiments–Center for Integrated Nanotechnologies under User Proposals #2019BC0126 and 2121BC0097; Electron microscopy–OSU Center for Electron Microscopy and Analysis (OSU CEMAS). Computations–the Ohio Supercomputing Center under User Grants PAS0676, PAS0971. PMA also acknowledges support through the Independent Research/Development Program while serving at the U.S. National Science Foundation. This work was performed, in part, at the Center for Integrated

Nanotechnologies, an Office of Science User Facility operated for the U.S. Department of Energy (DOE) Office of Science. Sandia National Laboratories is a multimission laboratory managed and operated by National Technology & Engineering Solutions of Sandia, LLC, a wholly owned subsidiary of Honeywell International, Inc., for the U.S. DOE's National Nuclear Security Administration under contract DE-NA-0003525. Los Alamos National Laboratory, an affirmative action equal opportunity employer, is managed by Triad National Security, LLC for the U.S. Department of Energy's NNSA, under contract 89233218CNA000001. The views expressed in the article do not necessarily represent the views of the U.S. DOE or the United States Government.

F. References

[1] O Benafan, GS Bigelow, AW Young, "Shape Memory Materials Database Tool—A Compendium of Functional Data for Shape Memory Materials," Adv. Eng. Mater. 22(7): 1901370–1901370 (2020). doi: 10.1002/adem.201901370.

[2] O Benafan, MR Moholt, M Bass, JH Mabe, D. E. Nicholson, F. T. Calkins, "Recent Advancements in Rotary Shape Memory Alloy Actuators for Aeronautics," *Shape Mem. Superelasticity* 5(4): 415–428 (2019). doi: 10.1007/s40830-019-00260-3.

[3] MH Elahinia, M Hashemi, M Tabesh, SB Bhaduri, "Manufacturing and processing of NiTi implants: A Review," *Prog. Mater. Sci.* 57(5): 911–946 (2012). doi: 10.1016/j.pmatsci.2011.11.001.

[4] J Mohd Jani, M Leary, A Subic, MA Gibson, "A review of shape memory alloy research, applications and opportunities," *Mater. Des.* 56: 1078–1113 (2014). doi: 10.1016/j.matdes.2013.11.084.

[5] J Van Humbeeck, "Shape memory alloys: A material and a technology," *Adv. Eng. Mater.* 3(11): 837–850 (2001). doi: 10.1002/1527-2648(200111)3:11<837::AID-ADEM837>3.0.CO;2-0.

[6] J Frenzel, EP George, A Dlouhy, C Somsen, MFX Wagner, G Eggeler, "Influence of Ni on martensitic phase transformations in NiTi shape memory alloys," *Acta Mater.* 58(9): 3444–3458 (2010). doi: 10.1016/j.actamat.2010.02.019.

[7] K Gall and HJ Maier, "Cyclic deformation mechanisms in precipitated NiTi shape memory alloys," *Acta Mater.* 50(18): 4643–4657 (2002). doi: 10.1016/S1359-6454(02)00315-4.

[8] J Khalil Allafi, X Ren, G Eggeler, "The mechanism of multistage martensitic transformations in aged Ni-rich NiTi shape memory alloys," *Acta Mater.* 50(4): 1359–6454 (2002). doi: 10.1016/S1359-6454(01)00385-8.

[9] J Ma, I Karaman, RD Noebe, "High temperature shape memory alloys," *Int. Mater. Rev.* 55(5): 257–315 (2010). doi: 10.1179/095066010X12646898728363.

[10] K Otsuka and X Ren, "Physical metallurgy of Ti-Ni-based shape memory alloys," *Prog. Mater. Sci.* 50(5): 511–678 (2005). doi: 10.1016/j.pmatsci.2004.10.001.

[11] M Rahim *et al.*, "Impurity levels and fatigue lives of pseudoelastic NiTi shape memory alloys," *Acta Mater.* 61(10): 3667–3686 (2013). doi: 10.1016/j.actamat.2013.02.054.

[12] I Karaman, H Ersin Karaca, HJ Maier, ZP Luo, "The effect of severe marforming on shape memory characteristics of a Ti-rich NiTi alloy processed using equal channel angular extrusion," *Metall. Mater. Trans. A.* 34: 2527-2539 (2003). doi: 10.1007/s11661-003-0012-5.

[13] H Nakayama, K Tsuchiya, M Umemoto, "Crystal refinement and amorphisation by cold rolling in TiNi shape memory alloys," *Scr. Mater.* 44(8-9): 1781–85 (2001). doi: 10.1016/S1359-6462(01)00740-0.

[14] T Waitz, V Kazykhanov, HP Karnthaler, "Martensitic phase transformations in nanocrystalline NiTi studied by TEM," *Acta Mater.* 52(1): 137–147 (2004). doi: 10.1016/j.actamat.2003.08.036.

[15] J Michutta, MC Carroll, A Yawny, C Somsen, K Neuking, G Eggeler, "Martensitic phase transformation in Ni-rich NiTi single crystals with one family of Ni4Ti3precipitates," *Mater. Sci. Eng. A* 378(1-2) Spec. Issue: 152–156 (2004). doi: 10.1016/j.msea.2003.11.061.

[16] J Khalil-Allafi, A Dlouhy, G Eggeler, "Ni4Ti3-precipitation during aging of NiTi shape memory alloys and its influence on martensitic phase transformations," *Acta Mater.* 50(17): 4255–4274 (2002). doi: 10.1016/S1359-6454(02)00257-4.

[17] H Mori, H Fujita, M Fujita, “Electron irradiation induced amorphization at dislocations in NiTi,” *Jpn. J. Appl. Phys. Part 2 Lett.* 22(2): L94–L96 (1983). doi: 10.1143/jjap.22.l94.

[18] G Thomas, H Mori, H Fujita, R Sinclair, “Electron irradiation induced crystalline amorphous transitions in NiTi alloys,” *Scr. Metall.* 16(5): 589–592 (1982). doi: 10.1016/0036-9748(82)90276-9.

[19] JL Brimhall, HE Kissinger, AR Pelton, “The amorphous phase transition in irradiated NiTi alloy,” *Radiat. Eff.* 90(3-4): 241–258 (1985). doi: 10.1080/00337578508222535.

[20] DF Pedraza, “Mechanisms of the electron irradiation-induced amorphous transition in intermetallic compounds,” *J. Mater. Res.* 1(3): 425–441 (1986). doi: 10.1557/JMR.1986.0425.

[21] P Moine and C Jaouen, “Ion beam induced amorphization in the intermetallic compounds NiTi and NiAl,” *J. Alloys Compounds*, vol. 194, no. 2, 1993. doi: 10.1016/0925-8388(93)90022-F.

[22] PJ Maziasz, DF Pedraza, JP Simmons, NH Packan, “Temperature dependence of the amorphization of NiTi irradiated with Ni ions,” *J. Mater. Res.* 5(5): 932–941 (1990). doi: 10.1557/JMR.1990.0932.

[23] TB Lagrange and R Gotthard, “Microstructural evolution and thermo-mechanical response of Ni ion irradiated TiNi SMA thin films,” *Optoelec. Adv. Mater.-Rapid ComM*, 5(1): (2003).

[24] T Lagrange, R Schäublin, DS Grummon, C Abromeit, R Gotthardt, “Irradiation-induced phase transformation in undeformed and deformed NiTi shape memory thin films by high-energy ion beams,” *Philos. Mag.* 85(4-7) Spec. Issue: 577–587 (2005). doi: 10.1080/02678370412331320107.

[25] G Laplanche, J Pfetzing-Micklich, G Eggeler, “Sudden stress-induced transformation events during nanoindentation of NiTi shape memory alloys,” *Acta Mater.* 78: 144–160 (2014). doi: 10.1016/j.actamat.2014.05.061.

[26] G Laplanche, J Pfetzing-Micklich, G Eggeler, “Orientation dependence of stress-induced martensite formation during nanoindentation in NiTi shape memory alloys,” *Acta Mater.* 68: 19–31 (2014). doi: 10.1016/j.actamat.2014.01.006.

[27] J Pfetzing-Micklich *et al.*, “Nanoindentation of a pseudoelastic NiTiFe shape memory alloy,” *Adv. Eng. Mater.* 12(1–2): 13–19 (2010). doi: 10.1002/adeM200900266.

[28] P Hosemann, JG Swadener, D Kiener, GS Was, SA Maloy, N Li, “An exploratory study to determine applicability of nano-hardness and micro-compression measurements for yield stress estimation,” *J. Nucl. Mater.* 375(1): 135–143 (2008). doi: 10.1016/j.jnucmat.2007.11.004.

[29] P Hosemann *et al.*, “Nanoindentation on ion irradiated steels,” *J. Nucl. Mater.* 389(2): 239–247 (2009). doi: 10.1016/j.jnucmat.2009.02.026.

[30] DM Norfleet *et al.*, “Transformation-induced plasticity during pseudoelastic deformation in Ni-Ti microcrystals,” *Acta Mater.* 57(12): 3549–3561 (2009). doi: 10.1016/j.actamat.2009.04.009.

[31] J Pfetzing-Micklich *et al.*, “On the crystallographic anisotropy of nanoindentation in pseudoelastic NiTi,” *Acta Mater.* 61(2): 602–616 (2013). doi: 10.1016/J.ACTAMAT.2012.09.081.

[32] J Pfetzing-Micklich, R Ghisleni, T Simon, C Somsen, J. Michler, G Eggeler, “Orientation dependence of stress-induced phase transformation and dislocation plasticity in NiTi shape memory alloys on the micro scale,” *Mater. Sci. Eng. A* 538: 265–271 (2012). doi: 10.1016/j.msea.2012.01.042.

[33] K Gall, H Sehitoglu, YI Chumlyakov, IV Kireeva, “Tension-compression asymmetry of the stress-strain response in aged single crystal and polycrystalline NiTi,” *Acta Mater.* 47(4): 1203-1217 (1999). doi: 10.1016/S1359-6454(98)00432-7.

[34] K Hattar, DC Bufford, DL Buller, “Concurrent in situ ion irradiation transmission electron microscope,” *Nucl. InstruM Methods Phys. Res. Sect. B Beam Interact. Mater. At.* 338: 56–65 (2014). doi: 10.1016/j.nimb.2014.08.002.

[35] JF Ziegler, MD Ziegler, JP Biersack, “SRIM - The stopping and range of ions in matter (2010),” *Nucl. InstruM Methods Phys. Res. Sect. B Beam Interact. Mater. At.* 268(11-12): 1818–1823 (2010). doi: 10.1016/j.nimb.2010.02.091.

[36] J Zhu, D Wang, Y Gao, TY. Zhang, Y Wang, “Linear-superelastic metals by controlled strain release via nanoscale concentration-gradient engineering,” *Mater. Today* 33(10): 17–23 (2020). doi: 10.1016/j.mattod.2019.10.003.

[37] C Domb and J Lebowitz, Eds., *Phase Transitions and Critical Phenomena, Vol. 18 - 1st Ed.*, 1st ed. Elsevier (2000). ISBN: 9780080538754.

[38] S Plimpton, “Fast Parallel Algorithms for Short-Range Molecular Dynamics,” *J. Comput. Phys.* 117(1): 1–19 (1995). doi: 10.1006/jcph.1995.1039.

[39] W-S Ko, B Grabowski, J Neugebauer, “Development and application of a Ni-Ti interatomic potential with high predictive accuracy of the martensitic phase transition,” *Phys. Rev. B* 93=2(13): 134107 (2015). doi: 10.1103/PhysRevB.92.134107.

[40] A Stukowski, “Visualization and analysis of atomistic simulation data with OVITO–the Open Visualization Tool,” *Model. Simul. Mater. Sci. Eng.* 18(1): 015012 (2010). doi: 10.1088/0965-0393/18/1/015012.

[41] J Zupanc, N Vahdat-Pajouh, E Schäfer, “New thermomechanically treated NiTi alloys - a review,” *Int. Endod. J.* 51(10): 1088–1103 (2018). doi: 10.1111/iej.12924.

[42] S Zaefferer and NN Elhami, “Theory and application of electron channelling contrast imaging under controlled diffraction conditions,” *Acta Mater.* 75: 20–50 (2014). doi: 10.1016/j.actamat.2014.04.018.

[43] SJ Zinkle, “Radiation-induced effects on microstructure,” in *Comprehensive Nuclear Materials*, vol. 1. Elsevier Ltd (2012) 65–98. doi: 10.1016/B978-0-08-056033-5.00003-3.

[44] A Reichardt *et al.*, “In situ micro tensile testing of He +2 ion irradiated and implanted single crystal nickel film,” *Acta Mater.* 100: 147-154 (2015). doi: 10.1016/j.actamat.2015.08.028.

[45] C Lu *et al.*, “Direct Observation of Defect Range and Evolution in Ion-Irradiated Single Crystalline Ni and Ni Binary Alloys,” *Sci. Rep.* 6(1): 19994–19994 (2016). doi: 10.1038/srep19994.

[46] RZ Valiev, RK Islamgaliev, IV Alexandrov, “Bulk nanostructured materials from severe plastic deformation,” *Prog. Mater. Sci.* 45(2): 103–189 (2000). doi: 10.1016/S0079-6425(99)00007-9.

[47] AT Motta, “Amorphization of intermetallic compounds under irradiation – A review,” *J. Nucl. Mater.* 244(3): 227–250 (1997). doi: 10.1016/S0022-3115(96)00740-4.